Threshold plasticity of hybrid Si-VO_2 microring resonators

Zhi Wang[1], Qiang Li[1], Ziling Fu[1], Andrew Katumba[2], Florian Denis-le Coarer[3], Damien Rontani[3], Marc Sciamanna[3], Peter Bienstman[2]

[1] Institute of Optical Information, Key Laboratory of Luminescence and Optical Information, Ministry of Education, Beijing Jiaotong University, Beijing 100044, China

[2] Photonic Research Group, Ghent University - IMEC, Ghent 9052, Belgium

[3] Chair in Photonics, LMOPS EA 4423 laboratory, CentraleSupelec,Univ. of Paris-Saclay, and Univ. of Lorraine, Metz 57070, France

zhiwang@bjtu.edu.cn (Z. Wang); peter.bienstman@ugent.be (P. Bienstman)

Abstract: We theoretically simulate the threshold plasticity of a high-Q-factor silicon-on-insulator microring resonator integrated with VO_2. The proposed © 2020 The Author(s) rform excitatory and inhibitory learning by tuning the initial working condition.

OCIS codes: 200.4700 Optical neural systems; 230.1150 All-optical devices; 230.3120 Integrated optics devices.

1. Introduction

Silicon-on-insulator (SOI) microring resonators are small-size passive devices and can be integrated on-chip. The high-Q SOI-microring resonator can exhibit class II neural excitability if it is pumped by sufficiently high input powers with a wavelength close to the resonance of the cavity [1, 2]. Threshold plasticity [3], which means the neural system learns by changing threshold rather than weights, is a candidate for learning of spiking neurons, and it is simpler and more amenable to hardware implementation. VO_2 is a phase change material that exhibits reversible semiconductor-to-metal transition (SMT). The SMT in VO_2 results in a large change in near-infrared transmission and refractive index, and it can be triggered by many different stimuli, such as temperature, electric field and optical excitation [4]. Hysteresis is a very important phase transition property for VO_2, and broad hysteresis could be useful in optical memory devices [5, 6].

In this paper, we propose to implement the threshold plasticity of nonlinear microring resonators by depositing a thin VO_2 film on top, as shown in Fig. 1(a). The simulations illustrating the concepts of this paper are performed with the nonlinear circuit simulator Caphe [7]. We demonstrate that our architecture can realize excitatory and inhibitory learning behavior.

2.N onlinear microring resonator with VO_2

The excitable microring is based on the cooperative effects of free-carrier dispersion (FCD) and the thermo-optic (TO) effect which induce a blueshift and redshift of the resonance wavelength, respectively. The coupled mode theory (CMT) model of a microring can correctly describe a wide range of nonlinear dynamics [1]. By integrating VO_2 on top of the ring, the SMT can be harnessed to introduce a significant change in absorption and effective index. The frequency shift induced by TO, FCD, two-photon absorption (TPA) effect and SMT is

$$\delta\omega_{nl} = -\frac{\omega_r}{n_g}\left[\frac{dn_{si}}{dT}\Delta T + \frac{dn_{si}}{dN}N + \frac{cn_2\Gamma_{TPA}|a|^2}{n_g V_{TPA}} + \frac{dn_{SMT}}{dT}\zeta\Delta T\right], \quad (1)$$

where ω_r is the resonance frequency of the cavity, n_{Si} is the refractive index of bulk silicon, a is the mode amplitude, ΔT is the mode-averaged temperature difference with the surroundings, N is the concentration of free carriers, dn_β/dT is effective index change coefficient by nonlinear effect β, c is the speed of light in vacuum, Γ_{TPA} is the TPA confinement factor, V_{TPA} is the TPA effective volume, n_2 is the Kerr nonlinear index, L is the length of VO_2, $\zeta = L/(2\pi R)$ is the ratio of VO_2 length to microring circumference, $n_g = (1-\zeta)n_{Si} + \zeta n_{SMT}(T_0)$ is the average group index of microring, and T_0 is the initial temperature. The loss rate induced by SMT is $\gamma_{SMT} = \zeta\alpha c / n_g$ [8], and α is the loss of Si-VO_2 waveguide. We assume that the linear absorption loss fraction induced by VO_2 is $\eta_{SMT,lin}$ =0.4. The parameters of VO_2 using in our simulation are extracted from Ref. [9]. The thickness of VO_2 on top of the microring is 80nm. When VO_2 is in the fully insulating phase (30°C), the designed Si-VO_2 waveguide supports a TE-mode with effective index of n_{eff}=2.691 and propagation loss of α=2.98dB/um, as shown in Fig.1 (b); when VO_2 is fully in the metallic state (85°C), the designed Si-VO_2 waveguide supports a TE-mode with effective index of n_{eff}=2.351 and propagation loss of α=3.49dB/um, as shown in Fig.1 (c).

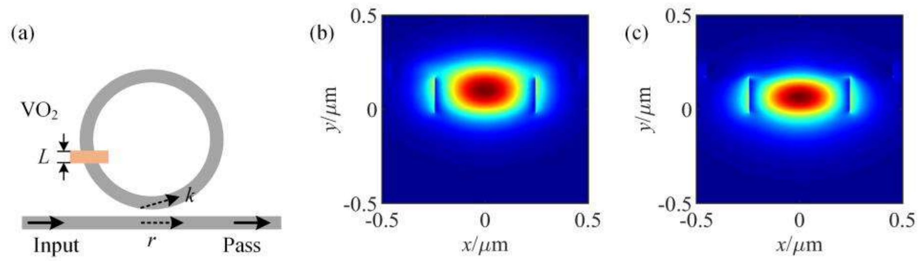

Fig. 1. (a) Schematic diagram of microring integrated with VO_2; the simulated electric field intensity of the Si-VO_2 waveguide when the VO_2 is in the (b) insulating and (c) metallic state

The hysteresis of VO_2 can be described by Prandtl-Ishlinskii (PI) model [10]. In this paper, we define a PI model of VO_2 and give a state-of-the art overview of the dynamic analysis of ring integrated with VO_2. As shown in Fig. 2 (a) and (b), by starting with the fully insulating state (20℃), we heat up VO_2 to various temperatures then cool back to the insulating state. The cooling and heating processes take different paths which are found in many measurements [5, 6, 11]. Therefore, the information is stored in the phase transition of VO_2, which means it can be used as a memory material.

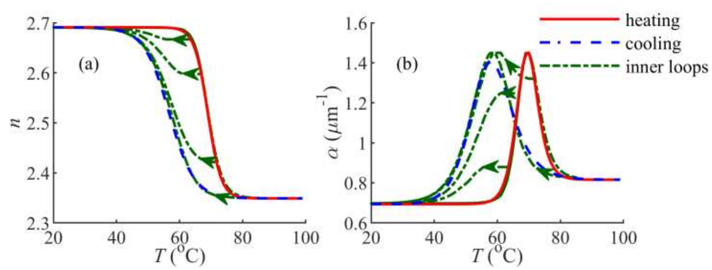

Fig. 2. The hysteresis of (a) effective index and (b) loss change of Si-VO_2 waveguide describing by temperature

The effective index and loss of Si-VO_2 waveguide highly depend on the initial temperature T_0, as shown in Fig. 2. The effective index exhibits a monotonous change with the temperature; the loss increases first then decreases while temperature increases. As shown in Fig. 3 (a) and (b), when T_0 is changed from 54℃ to 66℃, the threshold of the microring increases with increasing temperature; when T_0 is changed from 70℃ to 82℃, the threshold decreases with increasing temperature. This corresponds to the change of loss of Si-VO_2 waveguide shown in Fig. 2(b).

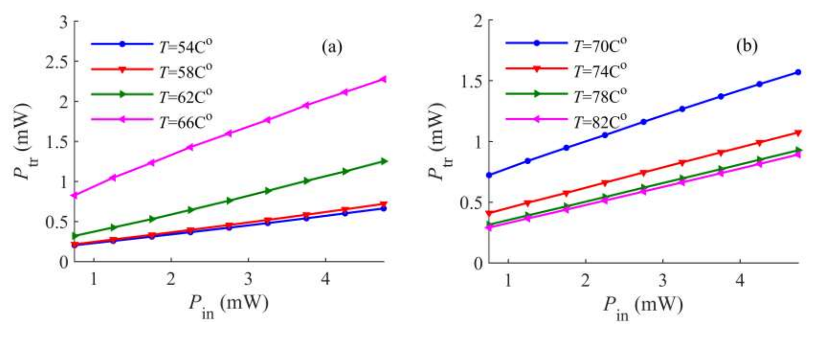

Fig. 3. Threshold of optical spiking ring changes with different power of pump light at different initial temperature T_0. $\Delta\lambda$=100pm, t_{tr}=10ns, ζ=0.0004.

By sending pulses with varying P_{tr}-height (amplitude of trigger pulse), we can get the threshold change of microring, as shown in Fig. 4. The trigger pulses are square pulses with 10ns width, the wavelength of trigger light is the same as the pump light with wavelength detuning $\Delta\lambda$=100pm, and the range of the initial temperature T_0 is from 54℃ to 82℃. When T_0 is changed from 54℃ to 62℃, the threshold of microring increases with the increasing P_{tr} due to the increasing loss induced by the SMT, as shown in Fig. 4(a)-(c). When the ring works at 66℃, with the increasing amplitude of trigger light, the threshold of microring increases at first then decreases, as shown in Fig. 4 (d). This is because the loss induced by the SMT increases first then decreases. When T_0 is changed from 70℃ to 82℃, the threshold decreases with the increasing amplitude of trigger light because of the decreasing loss, as shown in Fig. 4(e)-(h).

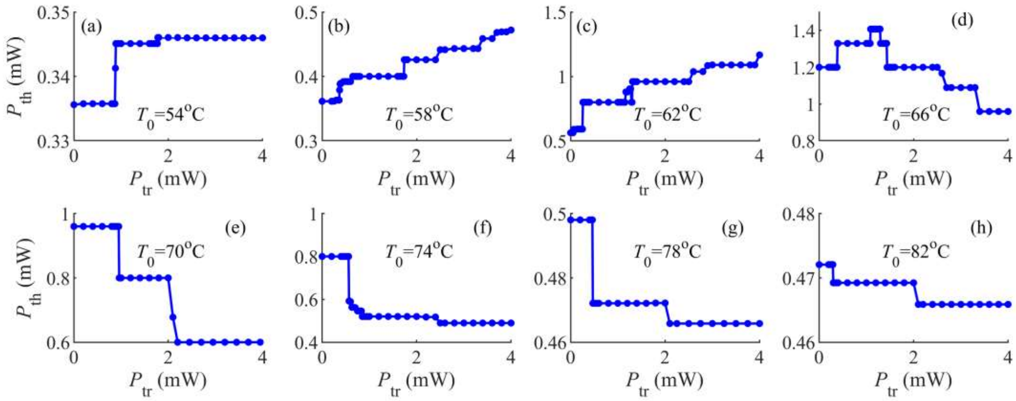

Fig.4. Threshold of optical spiking ring changes different amplitude of trigger pulse P_{tr} at different initial temperature T_0. P_{in}=2mW, ζ=0.0004, $\Delta\lambda$=100pm, t_{tr}=10ns

3. Conclusion

In conclusion, we numerically simulate the threshold plasticity of a high-Q microring integrated with VO_2. The proposed architecture can perform excitatory and inhibitory learning behavior by tuning the initial temperature, as well as electrical bias.

4. Acknowledgements

This work was supported in part by the National Natural Science Foundation of China under Grant 61571035 and China Scholarship Council.

5. References

1. T. Van Vaerenbergh, M. Fiers, P. Mechet, T. Spuesens, R. Kumar, G. Morthier, B. Schrauwen, J. Dambre, and P. Bienstman, "Cascadable excitability in microrings," Opt. Express **20**, 20292 (2012).
2. F. D.-L. Coarer, M. Sciamanna, A. Katumba, M. Freiberger, J. Dambre, P. Bienstman, and D. Rontani, "All-Optical Reservoir Computing on a Photonic Chip Using Silicon-Based Ring Resonators," IEEE J. Sel. Top. Quantum Electron. **24**, 7600108 (2018).
3. G. Tesauro, "A plausible neural circuit for classical conditioning without synaptic plasticity.," PNAS **85**(8), 2830–2833 (1988).
4. J. D. Ryckman, K. A. Hallman, R. E. Marvel, R. F. Haglund, and S. M. Weiss, "Ultra-compact silicon photonic devices reconfigured by an optically induced semiconductor-to-metal transition," Opt. Express **21**, 10753 (2013).
5. D. Y. Lei, K. Appavoo, F. Ligmajer, Y. Sonnefraud, R. F. Haglund, and S. A. Maier, "Optically-Triggered Nanoscale Memory Effect in a Hybrid Plasmonic-Phase Changing Nanostructure," ACS Photonics **2**, 1306–1313 (2015).
6. K. Ito, K. Nishikawa, and H. Iizuka, "Multilevel radiative thermal memory realized by the hysteretic metal-insulator transition of vanadium dioxide," Appl. Phys. Lett. **108**, 053507 (2016).
7. M. Fiers, T. Van Vaerenbergh, K. Caluwaerts, D. Vande Ginste, B. Schrauwen, J. Dambre, and P. Bienstman, "Time-domain and frequency-domain modeling of nonlinear optical components at the circuit-level using a node-based approach," J. Opt. Soc. Am. B **29**, 896 (2012).
8. B. Pile and G. Taylor, "Small-signal analysis of microring resonator modulators," Opt. Express **22**(12), 14913–14928 (2014).
9. J. B. Kana Kana, G. Vignaud, A. Gibaud, and M. Maaza, "Thermally driven sign switch of static dielectric constant of VO_2 thin film," Opt. Mater. **54**, 165–169 (2016).
10. J. Zhang, E. Merced, N. Sepúlveda, and X. Tan, "Modeling and inverse compensation of hysteresis in vanadium dioxide using an extended generalized Prandtl–Ishlinskii model," Smart. Mater. Struct. **23**, 125017 (2014).
11. L. Fan, Y. Chen, Q. Liu, S. Chen, L. Zhu, Q. Meng, B. Wang, Q. Zhang, H. Ren, and C. Zou, "Infrared Response and Optoelectronic Memory Device Fabrication Based on Epitaxial VO_2 Film," ACS Appl. Mater. Interfaces **8**, 32971–32977 (2016).